remote sensing

Article

Quantifying the Influences of Driving Factors on Vegetation EVI Changes Using Structural Equation Model: A Case Study in Anhui Province, China

Zhengnan Gu [1,2,3,4], Zhen Zhang [1,2,*], Junhua Yang [2] and Leilei Wang [1,3,4]

1 School of Geomatics, Anhui University of Science and Technology, Huainan 232001, China
2 State Key Laboratory of Cryospheric Science, Northwest Institute of Eco-Environment and Resources, Chinese Academy Sciences, Lanzhou 730000, China
3 Key Laboratory of Aviation-Aerospace-Ground Cooperative Monitoring and Early Warning of Coal Mining-Induced Disasters of Anhui Higher Education Institutes, Anhui University of Science and Technology, Huainan 232001, China
4 Coal Industry Engineering Research Center of Mining Area Environmental and Disaster Cooperative Monitoring, Anhui University of Science and Technology, Huainan 232001, China
* Correspondence: zhangzhen@aust.edu.cn

Abstract: Vegetation cover is important to the stability of regional ecosystems and is a focus of research on the relationship between natural and human environments. Although some studies have investigated the association between changes in vegetation cover and various influencing factors, these have shortcomings in quantifying direct and indirect effects. In this study, MOD13Q1 enhanced vegetation index (EVI) data for Anhui Province, China, were acquired between 2000 and 2020. The univariate linear regression, coefficient of variation and Hurst index methods were used to analyze spatial and temporal trends and fluctuations in the EVI between 2000 and 2020 and predict future trends. The impact of land-use change on EVI change was explored using 2000 and 2020 land-use data. Finally, a structural equation model (SEM) was used to quantify the effects of topography, annual average temperature, annual precipitation and human activity changes on EVI variation in Anhui Province. The results show that (1) from 2000 to 2020, the overall EVI in Anhui Province showed a fluctuating trend that increased at a rate of $0.0181 \cdot 10a^{-1}$, and 67.1% of the study area showed a greening trend. The EVI was relatively stable in most regions, with regions of fluctuating EVI being mostly affected by urbanization. For a period after 2020, the overall EVI change will exhibit anti-sustainability and will likely decrease. (2) Among the regions of EVI increase, 72.2% had no change in land-use type, while 10.8% and 6.6% changed to farmland and woodland land uses, respectively. Among the regions where EVI decreased, 69.9% had no change in land-use type, while 13.7% changed from farmland to construction land. (3) Overall, human activity change was the main influence on EVI change, which was mainly reflected in the negative impacts of accelerated urbanization. Topography had direct and indirect effects on EVI variations in Central and Southern Anhui. Annual precipitation change had a stronger impact on EVI variation in Northern and Central Anhui than in Southern Anhui, while annual average temperature change had a small impact in the entire province. Compared with other study methods, SEM provides a new approach to quantifying the influences of vegetation cover dynamics. In addition, the results of this study have important implications for ecological environmental protection and sustainable development in Anhui Province.

Keywords: enhanced vegetation index; spatial and temporal variations; structural equation model; driving factors; human activity; urbanization

check for updates

Citation: Gu, Z.; Zhang, Z.; Yang, J.; Wang, L. Quantifying the Influences of Driving Factors on Vegetation EVI Changes Using Structural Equation Model: A Case Study in Anhui Province, China. *Remote Sens.* **2022**, *14*, 4203. https://doi.org/10.3390/rs14174203

Academic Editors: Chunbo Huang, Ximing Ren and Jia Sun

Received: 13 June 2022
Accepted: 23 August 2022
Published: 26 August 2022

1. Introduction

Vegetation is the main component of the terrestrial ecosystem and the center of its material and energy cycles. It provides ecological functions such as soil improvement and air purification [1,2]. Therefore, it plays a significant role in maintaining regional ecosystem stability and regulating the climate [3]. To a certain extent, vegetation dynamics can respond to the natural environment and human activities. The general pattern of vegetation distribution is determined by long-term climate change. Topography affects the spatial distribution of vegetation by influencing the spatial distributions of light, temperature and precipitation [4]. Human activities directly or indirectly affect the dynamic changes of local vegetation [5,6]. Therefore, monitoring the dynamic evolution of regional vegetation and studying its relationships with changes in the natural environment and human activities are important in environmental protection and decision-making.

The development of remote sensing technology, especially high-spatial and -temporal-resolution hyperspectral images, has facilitated the large-scale monitoring of vegetation dynamics. Remote sensing images have been widely applied to study surface vegetation changes as they have a wide monitoring range and labor- and material-saving features [7,8]. Vegetation indexes can measure vegetation growth under certain conditions, so they are often used to monitor vegetation dynamics, such as the normalized difference vegetation index (NDVI), enhanced vegetation index (EVI), perpendicular vegetation index (PVI), ratio vegetation index (RVI) and green vegetation index (GVI), etc. In addition, there were also studies that generated a new index based on the combination of vegetation indexes with other indicators (evapotranspiration (ET), potential Evapotranspiration (PET), land surface temperature (LST), etc.) to study surface drought conditions [9,10], such as the drought severity index (DSI), temperature vegetation drought index (TVDI) and normalized vegetation supply water index (NVSWI), etc. By searching the status of vegetation dynamic change studies in recent years, NDVI and EVI are the most widely studied [11–13]. The NDVI can eliminate most of the effects associated with instrument calibration, sun angle, topography, clouds, shadows and changes in atmospheric conditions; however, it is inherently susceptible to saturation. Therefore, it has been improved and optimized to create the EVI, which can reflect vegetation growth changes more accurately in areas with high vegetation cover [14,15].

In recent years, there have been numerous in-depth studies on the factors influencing vegetation cover dynamics. Correlation analyses [16,17], multiple linear regression analyses [18], residual analyses [19,20] and geographical detector models [21,22] are the most widely used methods, while some studies have also used machine learning [23] (e.g., random forest) methods. From the perspective of driving factors, the impact of climate change on vegetation cover dynamics is the most widely studied [24,25]. It is commonly accepted that the main climatic factors affecting vegetation cover dynamics are temperature and precipitation [26,27]. With rapid economic development, human activities have intensified, making their effects on vegetation cover dynamics of wide concern. The effects of human activity factors, such as land-use change [28,29], population density [30], GDP (Gross Domestic Product) [31] and nighttime light [32], have been studied. In addition, some studies have focused on the effects of topographic factors, including elevation, slope and aspect, on vegetation cover dynamics [4,33]. However, the mechanisms influencing vegetation cover dynamics are intricate, and each influencing factor not only acts individually but may also interact with other factors. Traditional analysis methods only consider the direct effects of influencing factors on vegetation cover dynamics [34], which may sometimes be unrealistic. Therefore, it is important to quantify the direct and indirect influences on vegetation cover dynamics to determine the overall effect, which can inform regional environmental protection and decision-making.

The structural equation model (SEM) is a multivariate statistical method based on a covariance matrix, which is a multivariate analytical equation that includes a factor analysis and path analysis [35]. Moreover, SEM can deal with multiple independent and dependent variables at the same time [36] and, thus, identify the direct and indirect effects of independent variables on the dependent variable, thus obtaining the total effect [37,38]. In addition, SEM can also reflect the relationships between the effects of multiple variables [39]. Therefore, SEM may be a more effective method for impact factor analysis than traditional multivariate statistical methods (e.g., multiple linear regression). Shao et al. [40] explored the effects of topography, climate and vegetation changes on soil available nutrients based on SEM. Wang et al. [34] analyzed vegetation phenological characteristics based on NDVI and used SEM to explore the potential mechanisms of climate and soil factors on vegetation phenology in the Three-River Headwaters Region. However, few studies have applied SEM to analyse the influences on vegetation cover dynamics [41].

Anhui Province is an important grain production base in China. Changes in its vegetation cover are closely related to grain production. Therefore, studying the vegetation cover status of this region is crucial for China's food security. However, due to the special geographical location of Anhui Province, the topography and climate of southern, central and northern Anhui differ greatly. This has resulted in a poor zonal distribution of vegetation that creates challenges for research [42]. Accordingly, few studies have quantitatively analyzed the influences on vegetation cover dynamics in this region. As far as we know, Yao et al. [43] studied the vegetation dynamics in Anhui Province; however, they only considered the influence of topography on vegetation cover change and did not consider the influence of climate and human activity changes on vegetation cover change.

As a result, the main tasks of this study were to (1) analyze the characteristics of spatial and temporal variation in the EVI in Anhui Province from 2000 to 2020; (2) explore a coupled model of changes in land use and the EVI and (3) quantify the effects of changes in topography, climate (annual average temperature and annual precipitation) and human activity on EVI changes and explore the driving mechanisms. The results of the study provide a scientific basis for vegetation conservation, ecological environmental management and the sustainable development of Anhui Province.

2. Materials and Methods

2.1. Study Area

Anhui Province (29°41′–34°38′N, 114°54′–119°37′E; Figure 1) is located in East China and is an important part of the Yangtze River Delta. The terrain is composed of plains, hills and mountains and is generally high in the southwest and low in the northeast. Anhui Province has three natural geographical areas, namely, North Anhui Plain, Central Anhui (Central Anhui Hills) and South Anhui (South Anhui Mountains), and it spans three major water systems, namely, the Huaihe, Yangtze and Xin'an Rivers. It is situated in a climatic transition area where the Huaihe River forms a boundary between a warm, temperate, semi-humid monsoon climate to the north and a subtropical, humid monsoon climate to the south. The monsoon is obvious; there are four distinct seasons, and natural disasters occur from time to time in the region. The annual average temperature is 15–18 °C. The average annual precipitation is 800–1800 mm, which falls more in the south than in the north and more on the mountains than on the plains and hills. Anhui Province is an important agricultural production base. Farmland is the primary land-use type, accounting for 55.38% of the province's area in 2020, being mainly in the north and central Anhui plain areas.

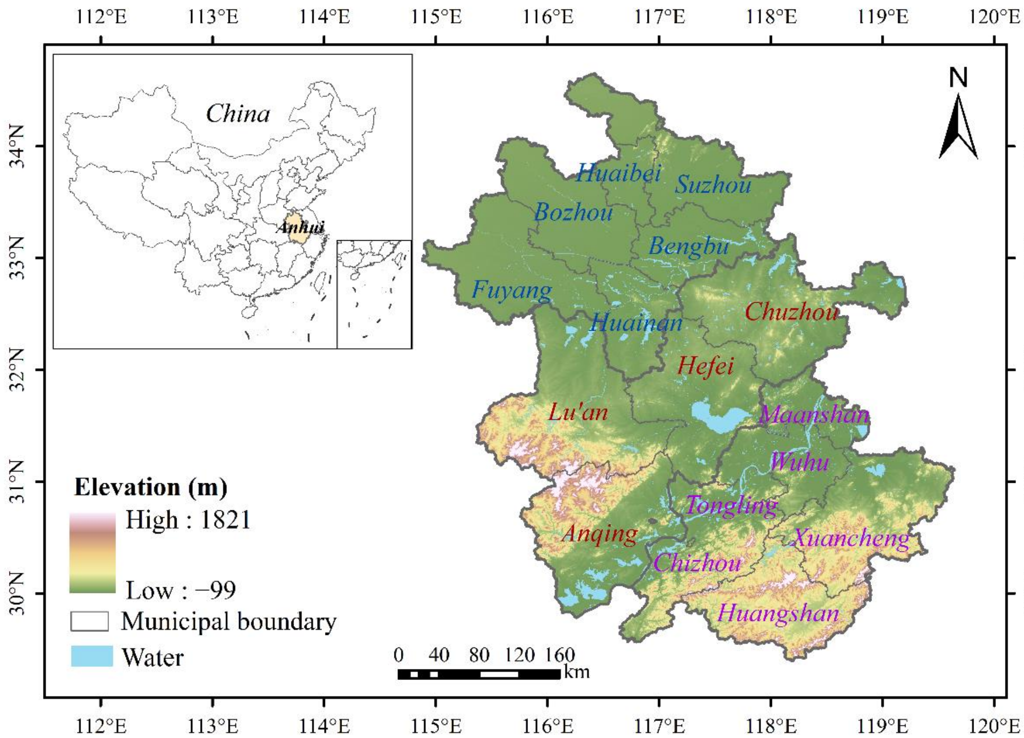

Figure 1. Elevation map of the Anhui Province study area. Note: Blue characters represent northern Anhui, red characters represent central Anhui and purple characters represent southern Anhui.

2.2. Data Acquisition and Processing

For this study, due to the temporal limitations of population density, nighttime light and land use data, the study period was 2000–2020. The data used include EVI as well as topographic, human activity and climate factors. The data are described in Table 1.

Table 1. Basic information of the study data.

Dataset		Temporal /Spatial Resolution	Period	Data Sources
EVI		16 d/250 m	2000–2020	MOD13Q1.006 Terra Vegetation Indices 16-Day Global 250 m (https://earthengine.google.com, accessed on 26 January 2022)
Topographic factors	Elevation	30 m	2000	SRTM DEM (https://earthexplorer.usgs.gov, accessed on 26 January 2022)
	Slope Aspect	30 m	2000	Derived from SRTM DEM
Human activity factors	Populationdensity	1 km	2000–2020	World population density map (https://www.worldpop.org, accessed on 26 January 2022)
	Nighttime light	500 m	2000–2018	An extended time series (2000–2018) of global NPP-VIIRS-like nighttime light data (https://doi.org/10.7910/DVN/YGIVCD accessed on 26 January 2022)
	Land use	1 km	2000/2020	Anhui land-use datasets (http://www.resdc.cn, accessed on 26 January 2022)
Climate factors	Annual average temperature	Monthly /1 km	2000–2020	Daily surface climate data for China (V3.0) (http://data.cma.cn, accessed on 26 January 2022)
	Annual precipitation	Monthly /1 km	2000–2020	Daily surface climate data for China (V3.0) (http://data.cma.cn, accessed on 26 January 2022)

2.2.1. EVI Data

In this study, MOD13Q1 EVI data acquired from 2000 to 2020 were used to study the long-term dynamics of vegetation in Anhui Province. The dataset has a spatial resolution of 250 m and a temporal resolution of 16 d. The data were obtained via online access to the Google Earth Engine (GEE, a data processing platform developed by Google, Carnegie Mellon University, and the United States Geological Survey) platform. The EVI annual maximum images from 2000 to 2020 were composited by the maximum value composite method, with Anhui Province clipped as the vector boundary.

2.2.2. Topographic Factors

The topographic factors used in this study include elevation, slope and aspect. They were extracted from the SRTM DEM. The aspects were reclassified as (1) shady slopes (0° to 45° or 315° to 360°), (2) semi-shady slopes (45° to 135°), (3) flat slopes (−1), (4) semi-positive slopes (225° to 315°) and (5) positive slopes (135° to 225°).

2.2.3. Human Activity Factors

The human activity factors used in this study include population density, nighttime light and land use. Population density data were obtained from the World Population Density Map published by WorldPop, which is the most accurate and reliable long-time-series dataset available. A comparative analysis of the long time series was not possible due to the mismatch between the nighttime light datasets acquired from two sensors, DMSP-OLS (1992–2013) and NPP-VIIRS (2012–present), which are published by the National Oceanic and Atmospheric Administration (NOAA). Therefore, this study used Chen et al.'s [44] extended time series (2000–2018) of global NPP-VIIRS-like nighttime light data, which has a good spatial pattern and temporal consistency that is similar to the composite NPP-VIIRS nighttime light data. Land use data in 2000 and 2020 were obtained from the Resource and Environment Science and Data Center. The slopes of the changes in population density from 2000 to 2020 and nighttime light from 2000 to 2018 were calculated using univariate linear regression. Land-use data were obtained for two years: 2000 and 2020. Pixels with land-use-type changes between 2000 to 2020 were recorded as 0, and those without changes were recorded as 1.

2.2.4. Climate Factors

The study used daily average temperature and daily precipitation data from 62 meteorological stations in and around Anhui Province. Daily data from each station were combined into monthly data, and ANUSPLIN software was used for interpolation at a spatial resolution of 1 km. The monthly raster data were further combined into annual data, and the trends in the annual average temperature and annual precipitation from 2000 to 2020 were calculated using the univariate linear regression method.

2.2.5. Data Processing

All data used in the study were projected onto the WGS_1984_UTM_Zone_50N coordinate system and resampled to 250 m (the same resolution as the EVI data) based on the nearest-neighbor method in ArcGIS 10.7. A total of 5346 sampling points were extracted by removing waterbodies, taking the center point of a 5 km × 5 km grid and removing the missing values. There were 1666 sampling points in northern Anhui, 2012 in central Anhui and 1668 in southern Anhui. Then, the values of each influencing factor at each sampling point were extracted to generate an attribute table.

2.3. Methods

2.3.1. Univariate Linear Regression

In this study, the spatial and temporal variations in EVI in Anhui Province were analyzed using univariate linear regression. The interannual variation at each pixel was calculated according to Equation (1):

$$slope = \frac{n\sum_{i=1}^{n} i f_{ci} - (\sum_{i=1}^{n} i)(\sum_{i=1}^{n} f_{ci})}{n\sum_{i=1}^{n} i^2 - (\sum_{i=1}^{n} i)^2} \tag{1}$$

where f_{ci} represents the EVI value of the pixel in year i, and n represents the study period. A slope > 0 means that the EVI had an increasing trend during the study period, while values < 0 indicate a decreasing trend. Finally, the significance of the EVI trend was tested by F-tests. Based on the results of the univariate linear regression and F-tests, the EVI trends in the study area were divided into five classes: Significant improvement ($slope > 0$, $p \leq 0.01$), improvement ($slope > 0$, $0.01 < p \leq 0.05$), basically stable ($p > 0.05$), degradation ($slope < 0$, $0.01 < p \leq 0.05$) and significant degradation ($slope < 0$, $p \leq 0.01$).

2.3.2. Coefficient of Variation

The coefficient of variation (CV) reflects the dispersion and fluctuation in a data distribution [45]. This study analyzed the stability of EVI changes in the study area based on the CV. Its equation is:

$$CV = \frac{1}{F}\sqrt{\frac{\sum_{i=1}^{n}(F_i - \overline{F})^2}{n}} 100\% \tag{2}$$

where n represents years, $\overline{F}$ represents the average EVI for n years, and F_i represents the EVI in year i. The greater the CV value, the more scattered the data, the greater the fluctuation and the lower the stability; conversely, a smaller CV means less dispersed data with lower fluctuation and higher stability.

The CVs were divided into five classes according to the natural breakpoint method: extremely low fluctuation ($0.02 \leq CV < 0.09$), low fluctuation ($0.09 \leq CV < 0.14$), moderate fluctuation ($0.14 \leq CV < 0.23$), high fluctuation ($0.23 \leq CV < 0.41$) and extremely high fluctuation ($0.41 \leq CV < 1.19$).

2.3.3. Hurst Index

The Hurst index can effectively describe the sustainability of a time series and, thus, predict its future trend. Therefore, it is frequently used in studies to predict vegetation cover changes [46]. In this study, the Hurst index of EVI change was calculated using a rescaled range (R/S) analysis according to the following process. For any time series $EVI_{(t)}$, $t = 1, 2, \ldots, n$, with any positive integer $\tau \geq 1$, the average value of the series is defined as:

$$\overline{EVI}_{(\tau)} = \frac{1}{\tau}\sum_{t=1}^{\tau} EVI_{(t)} \quad \tau = 1,\ 2,\ \ldots,\ \mathrm{n} \tag{3}$$

The cumulative deviation series $EVI_{(t,\tau)}$ is defined as:

$$EVI_{(t,\tau)} = \sum_{u=1}^{t}\left(EVI_{(u)} - \overline{EVI}_{(\tau)}\right) \quad 1 \leq t \leq \tau \tag{4}$$

The sequence of extreme differences $R_{(\tau)}$ is defined as:

$$R_{(\tau)} = \max_{1\leq t\leq\tau} EVI(t,\tau) - \min_{1\leq t\leq\tau} EVI(t,\tau) \quad \tau = 1,\ 2,\ \ldots,\ \mathrm{n} \tag{5}$$

The standard deviation series $S_{(\tau)}$ is defined as:

$$S_{(\tau)} = \left[\frac{1}{\tau}\sum_{t=1}^{\tau}\left(EVI_{(t)} - \overline{EVI}_{(\tau)}\right)^2\right]^{\frac{1}{2}} \tau = 1,\ 2,\ \ldots,\ \mathrm{n} \tag{6}$$

Calculation of the Hurst index:

$$\frac{R_{(\tau)}}{S_{(\tau)}} = (c\tau)^H \tag{7}$$

where H represents the Hurst index, c represents a constant and τ denotes the time series length. The following regularity exists for the Hurst index: (1) $0 < H < 0.5$, indicating that this time series is an anti-sustainability series, which means that the future trend in EVI will be opposite to the past trend. The smaller the H value, the stronger the anti-sustainability. (2) $H = 0.5$, indicating that this time series is a random series, which means that the future trend in EVI is independent of the past trend. (3) $0.5 < H < 1$, indicating that this time series is a positive sustainability series, which means that the future EVI trend will be consistent with the past trend. Higher H-values indicate stronger positive sustainability.

Then, the Hurst index and EVI trend significance results were superimposed according to the correspondence in Table 2 to obtain the classification results of EVI future trends.

Table 2. Classification of sustainability in EVI change.

Significance	**0 < H < 0.5**	**H = 0.5**	**0.5 < H < 1**
Significant degradation	Significant improvement		Significant degradation
Degradation	Improvement		Degradation
Basically stable	Basically stable	Uncertain	Basically stable
Improvement	Degradation		Improvement
Significant improvement	Significant degradation		Significant improvement

2.3.4. Structural Equation Model

Structural equation modelling (SEM) first originated in the social sciences [47] and has recently been applied to ecology [40,41]. In the following section, we will describe in detail the construction steps and modification process of SEM.

A reasonable conceptual model is essential when constructing an SEM [48]. In general, a number of assumptions about the relationships between variables are first made based on a review of the literature or a priori knowledge. Then, based on the model's fit optimality index, it is determined whether the study data fit the established model well. When the model fits poorly, it is necessary to reset it or remove and change insignificant paths based on theoretical assumptions and statistical results to improve the fit of the SEM and, thus, explain the relationships between the variables in the SEM.

In this study, topography and changes in human activity were defined as two classes of variables. Elevation, slope and aspect were used as observed variables in the topography. Population density change (Pd_change), nighttime light change (Ntl_change) and land-use change (Lu_change) were used as observed variables in the changes in human activity. Annual average temperature change (AaT_change) and annual precipitation change (AP_change) were added to the model as independent variables (observed variables) to construct an SEM of the factors influencing EVI change. We make the following assumptions: (1) Topography, annual average temperature change, annual precipitation change and human activity change all directly affect EVI variation; (2) topography can affect the changes in annual average temperature and annual precipitation; (3) topography can affect human activity changes; for example, high-altitude areas hinder human activities and, thus, the exploitation of natural resources. Based on the above assumptions, the conceptualized SEM was constructed as shown in Figure 2.

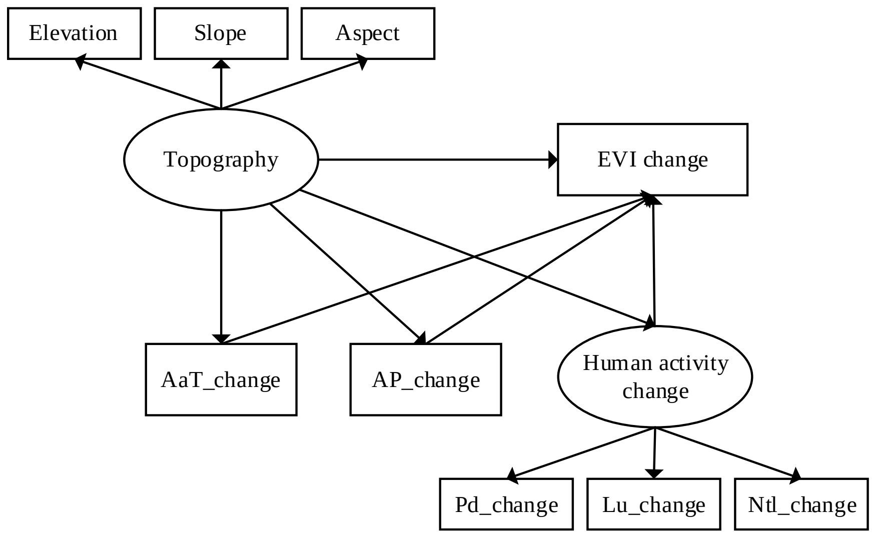

Figure 2. Conceptual structural equation model. Note: Rectangles represent observed variables, and ellipses represent latent variables. AaT_change = annual average temperature change; AP_change = annual precipitation change; Lu_change = land use change; Ntl_change = nighttime light change.

To determine the best-fitting model, five indicators were selected: CFI (Comparative Fit Index), GFI (Goodness of Fit Index), IFI (Incremental Fit Index), RMSEA (Root Mean Square Error of Approximation) and SRMR (Standardized Residual Mean Root). It is generally considered that the closer the CFI, IFI and GFI are to 1 and the closer RMSEA and SRMR are to 0, the better the model fit. Model construction, evaluation and correction were performed in AMOS 21 software (a standalone product in the SPSS (Statistical Product Service Solutions) Statistics package).

When each goodness of fit index of the model meets the requirements, the final fitted SEM is obtained. The corresponding standardized regression coefficients will be provided on each path. The direct influence is the path coefficient of the independent variable pointing directly to the dependent variable; the larger the path coefficient, the greater the influence; the indirect influence is the multiplication of the path coefficient of the influence of the independent variable on the intermediate variable and the path coefficient of the influence of the intermediate variable on the dependent variable; if there is more than one intermediate variable from the independent variable to the dependent variable, the indirect influence is the sum of each indirect influence path; the total influence is the sum of the direct influence and the indirect influence.

3. Results

3.1. Spatial and Temporal Variations in EVI in Anhui Province

3.1.1. Interannual Variation in EVI

The temporal trend in EVI in Anhui Province from 2000 to 2020 is shown in Figure 3. The average annual maximum EVI increased from 0.577 in 2000 to 0.621 in 2020, and the maximum and minimum EVIs occurred in 2011 (0.636) and 2003 (0.563). Overall, the interannual variation had a fluctuating increasing trend (Figure 3a). The slopes during the study period were $0.018{\cdot}10a^{-1}$, $0.0156{\cdot}10a^{-1}$, $0.0202{\cdot}10a^{-1}$ and $0.018{\cdot}10a^{-1}$ for the entire Anhui Province, northern Anhui, central Anhui, and southern Anhui, respectively (Figure 3a–d). Among them, the trends in EVI in the central and entire regions of Anhui Province were similar, with R^2 = 0.32381 (Figure 3a) and 0.3377 (Figure 3c), respectively. The increasing trend in EVI in northern Anhui was not significant (p = 0.138, Figure 3b), while that in southern Anhui was the most significant (p = 0.000, Figure 3d).

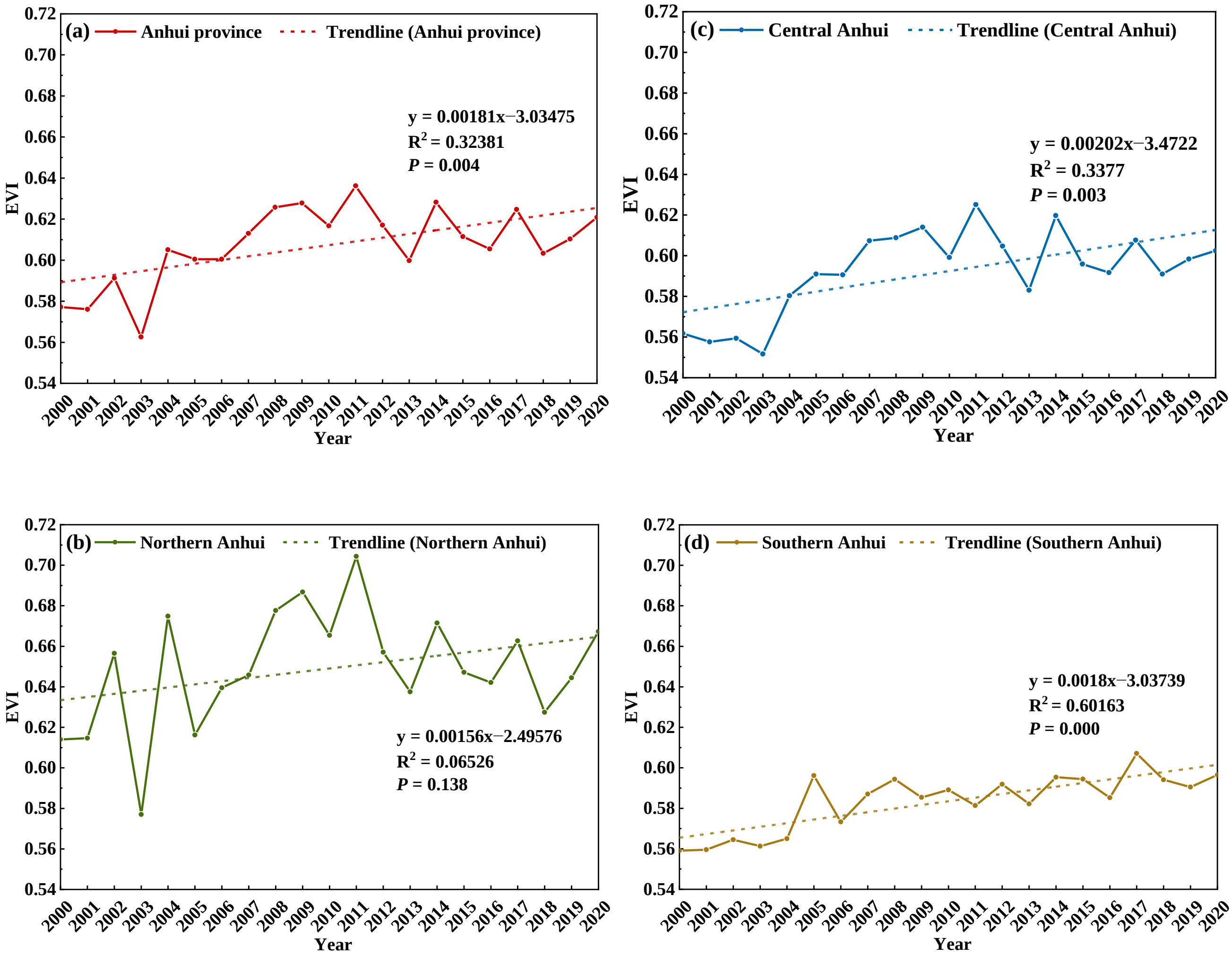

Figure 3. Temporal variations in annual maximum EVI mean during 2000–2020 in Anhui Province. (**a**) The entire Anhui Province and (**b**) Northern, (**c**) Central and (**d**) Southern Anhui.

3.1.2. Spatial Distribution Characteristics of EVI and Areas of Transfer

Based on the equal interval method, the EVI of Anhui Province was classified into five classes: 0–0.2, 0.2–0.4, 0.4–0.6, 0.6–0.8 and 0.8–1, representing extremely low, low, medium, high and extremely high vegetation cover, respectively. The EVI in Anhui Province showed a spatial distribution of being high in the north and south and low in the middle (Figure 4). From 2000 to 2020, Anhui Province was dominated by moderate-to-high vegetation cover, with EVIs $\geq$ 0.4 covering 96.5% and 94.4% of the area in 2000 and 2020, respectively (Table 3). Low and extremely low vegetation cover accounted for only 2.5% of Anhui Province, mainly occurring in construction land. Notably, from 2000 to 2020, the area of moderate vegetation cover decreased from 55.36% to 33.23%, while the low and extremely high vegetation cover areas increased from 3.17% and 0.89% to 5.16% and 5.60%, respectively. Changes in moderate and high vegetation cover represented the main forms of vegetation cover transfer in Anhui Province. The increase in low vegetation cover mainly came from the transfer of moderate vegetation cover, and the increase in extremely high vegetation cover mainly came from the transfer of high vegetation cover (Table 3).

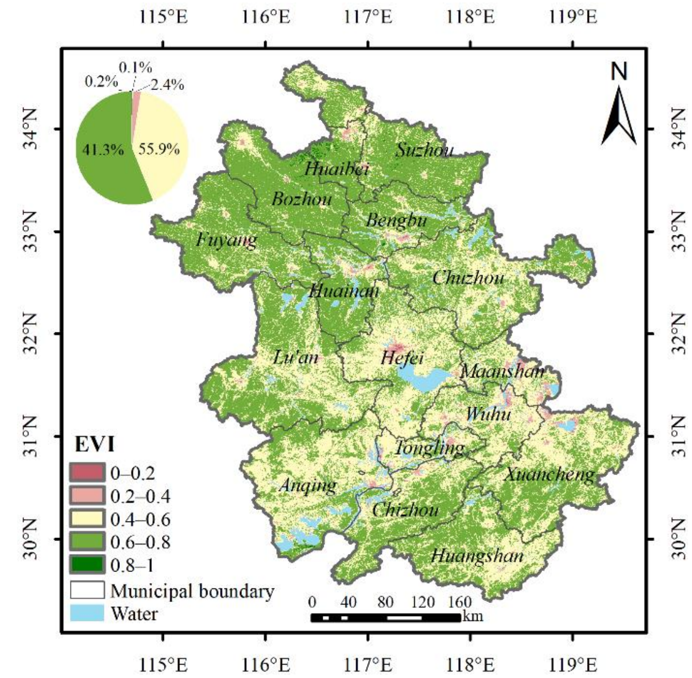

Figure 4. Spatial distribution of average EVI in Anhui Province during 2000–2020.

Table 3. Area transfer matrix of EVI in Anhui Province during 2000–2020 (km^2).

2000	**2020**					
	[0,0.2]	**[0.2,0.4]**	**[0.4,0.6]**	**[0.6,0.8]**	**[0.8,1]**	**Total**
[0,0.2]	117.31 (0.09%)	270.88 (0.20%)	48.13 (0.03%)	11.5 (0.01%)	1 (~0.00%)	448.82 (0.33%)
[0.2,0.4]	166 (0.12%)	1785.38 (1.33%)	1982.44 (1.47%)	328.38 (0.24%)	16.25 (0.01%)	4278.45 (3.17%)
[0.4,0.6]	201 (0.15%)	3774.13 (2.80%)	33,035.88 (24.52%)	35,755.25 (26.54%)	1820.88 (1.35%)	74,587.14 (55.36%)
[0.6,0.8]	70.5 (0.05%)	1097.75 (0.81%)	9495.13 (7.05%)	38,039.44 (28.23%)	5529.44 (4.11%)	54,232.26 (40.25%)
[0.8,1]	4.44 (~0.00%)	32.13 (0.02%)	212.38 (0.16%)	774 (0.58%)	172.31 (0.13%)	1195.26 (0.89%)
Total	559.25 (0.41%)	6960.27 (5.16%)	44,773.96 (33.23%)	74,908.57 (55.60%)	7539.88 (5.60%)	134,741.93 (100%)

3.1.3. Spatial Trend in EVI

The trend in EVI from 2000 to 2020 was calculated at the pixel scale and tested for significance (Figure 5). The results show that there was a decreasing EVI trend in 26.1% of the regions in Anhui Province and an increasing trend in 73.9% of the regions (Figure 5a). Among them, 64.2% of the regions had significant improvements in EVI, 19.4% of the regions had significant degradation (Figure 5b) and 12% of the regions remained largely stable.

From 2000 to 2020, the area of improved vegetation in Anhui Province (67.1%) was much larger than the area of degradation (20.9%); hence, the spatial trend in vegetation was dominated by improvement (Figure 5b). Among them, the areas of significantly degraded vegetation (19.4%) were mainly located in Fuyang, Bozhou and Huaibei cities in northern Anhui, Lu'an and Hefei cities in central Anhui and the urban belt of Wanjiang River, while areas with significantly improved vegetation (64.2%) were mainly located in the eastern north, western central and southern mountainous areas of Anhui.

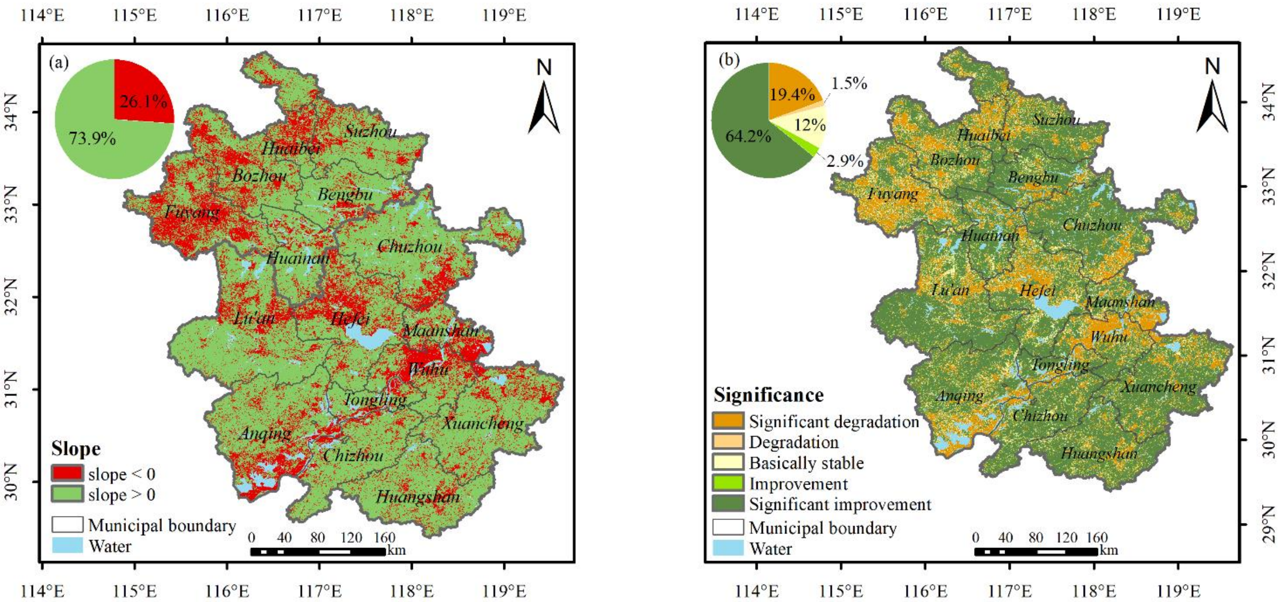

Figure 5. Spatial distribution of changes in EVI in Anhui Province during 2000–2020. (**a**) Slope of variation in EVI. (**b**) Spatial variation trend of EVI.

3.1.4. Stability of EVI Variations

The stability of EVI variations in Anhui Province from 2000 to 2020 is shown in Figure 6. The fluctuations in EVI variation in most regions (85.8% of the study area) were extremely low and low. The average CV in Anhui Province was about 0.11, indicating that there was little overall fluctuation in EVI over the past 21 years. Moderate and high fluctuations accounted for 13.9% of Anhui Province, mainly in construction land in the Wanjiang and Huaihe River basins and in Hefei city and other urban centers. The areas with extremely low and low fluctuations in EVI variation occurred mainly in non-urban areas, mainly in farmland and woodland.

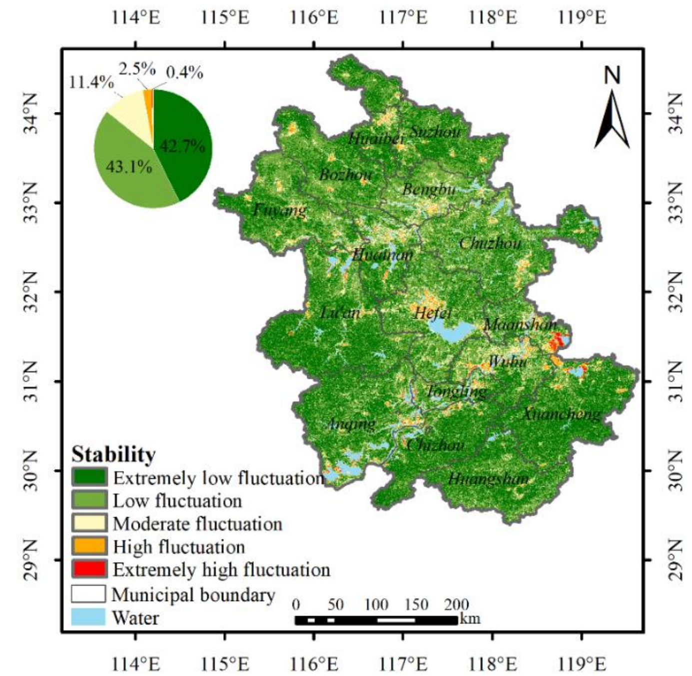

Figure 6. Stability of variations in EVI in Anhui Province during 2000–2020.

3.1.5. Sustainability of EVI Variations

The Hurst indexes of EVI variations in Anhui Province are shown in Figure 7a. Values of $H < 0.5$ occurred in most areas (72.3%) of Anhui Province, with an average value of 0.448, indicating that the overall EVI variation showed anti-sustainability, i.e., the trend in vegetation EVI variation in Anhui Province might be reversed in a period after 2020. Figure 7b shows a superimposed analysis of the Hurst index and EVI trends. The results show that the EVIs in Anhui Province would remain basically unchanged in 12% of the province and change in 88% in a period after 2020. Among them, areas with significant increases and decreases accounted for 29% and 54.5%, respectively.

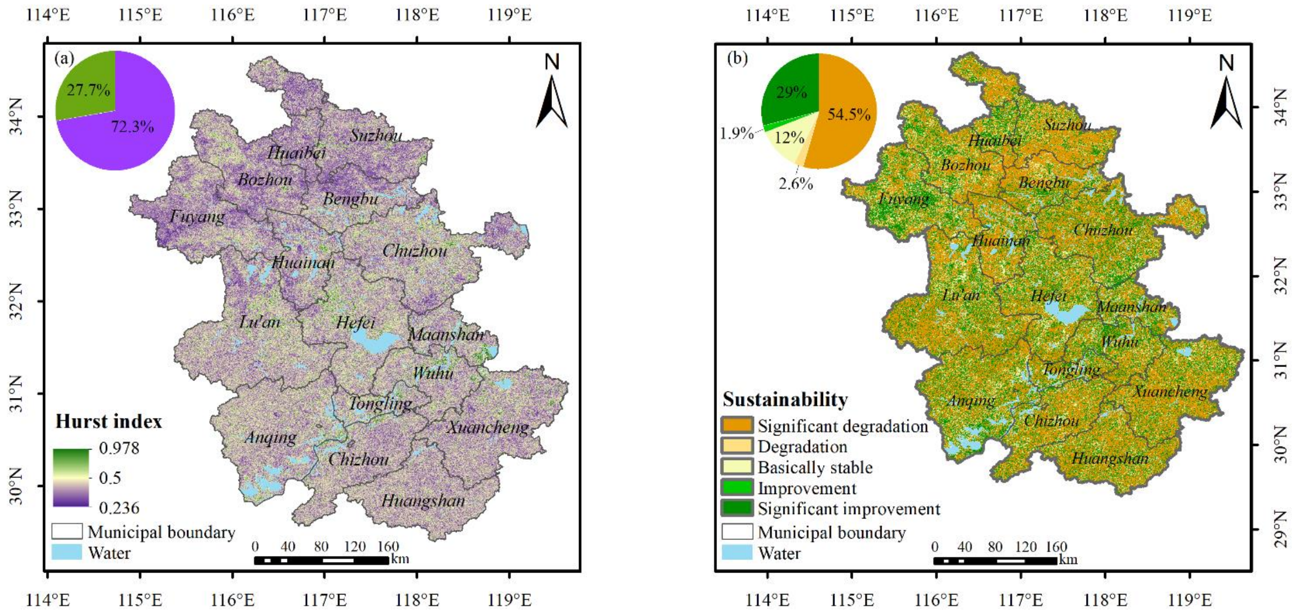

Figure 7. Sustainability of variations in EVI in Anhui Province during 2000–2020. (**a**) Hurst exponents of variation in the EVI. (**b**) Sustainability classification of variation in the EVI.

3.2. Superposition of EVI Variation and Land-Use Change in Anhui Province

We analyzed the spatial changes in land use types in Anhui Province using land-use data for the two periods of 2000 and 2020 (Figure 8). The results show that farmland was the dominant land-use type in Anhui Province, accounting for 57.8 and 55.4% of its area in 2000 and 2020, respectively, followed by woodland and construction land, with grassland and waterbodies accounting for lower proportions of the area. In addition, it can be seen from Figure 8 that the proportion of area occupied by construction land increased from 8% to 10.5% between 2000 and 2020, and there was a significant outward expansion. Combining this with data on the area transfer of each land-use type in Anhui Province in the period 2000–2020 (Table 4), we found that the majority of regional land-use types were unchanged. Unchanged areas occupied 96,889 km^2 (69.36% of the province). Among them, the type of land transferred from farmland was mainly construction land, accounting for an area of 11,191 km^2 (8.01%). A portion of construction land was also transferred to farmland, accounting for an area of 8085 km^2 (5.79%). This may be related to urban expansion and the intensive use of farmland.

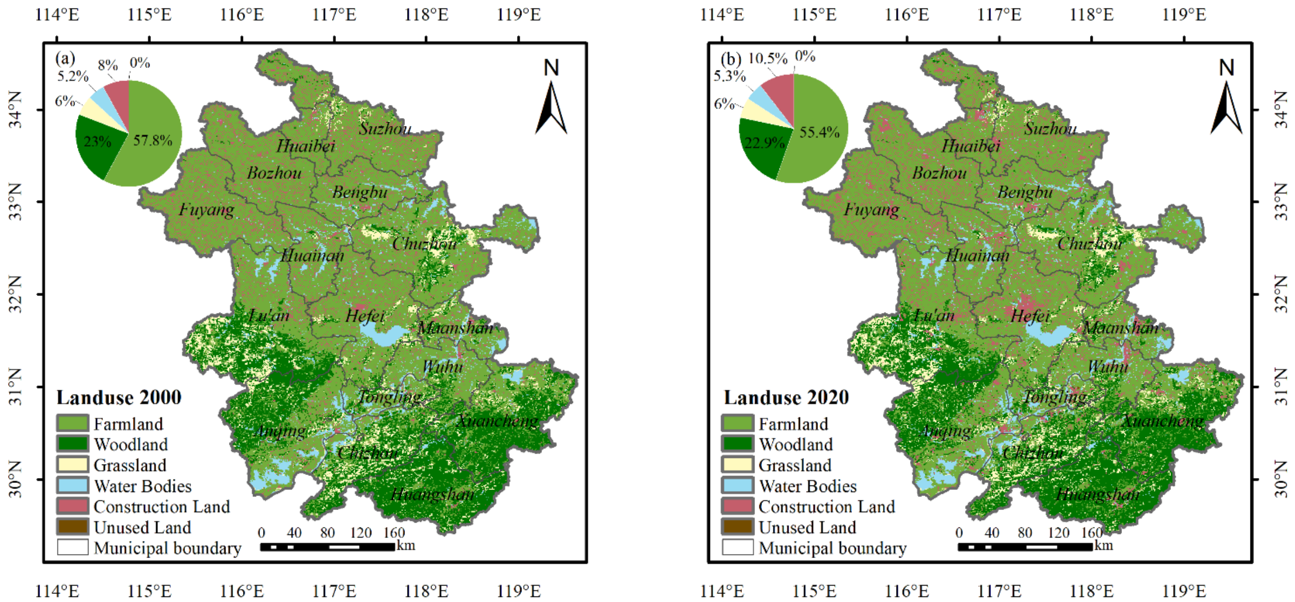

Figure 8. Land use in Anhui Province in (**a**) 2000 and (**b**) 2020.

Table 4. Area transfer matrix of land-use changes in Anhui Province during 2000–2020 (km^2).

2000	2020						
	Farmland	Woodland	Grassland	Waterbodies	Construction Land	Unused Land	Total
Farmland	61,135 (43.76%)	5062 (3.62%)	1233 (0.88%)	2189 (1.57%)	11,191 (8.01%)	18 (0.01%)	80,828 (57.85%)
Woodland	4878 (3.49%)	24,193 (17.32%)	2350 (1.68%)	249 (0.18%)	441 (0.32%)	2 (~0.00%)	32,113 (22.99%)
Grassland	1238 (0.89%)	2306 (1.65%)	4478 (3.21%)	123 (0.09%)	173 (0.12%)	3 (~0.00%)	8321 (5.96%)
Waterbodies	2030 (1.45%)	225 (0.16%)	147 (0.11%)	4537 (3.25%)	306 (0.22%)	0 (0.00%)	7245 (5.19%)
Construction land	8085 (5.79%)	209 (0.15%)	100 (0.07%)	252 (0.18%)	2546 (1.82%)	2 (~0.00%)	11,194 (8.01%)
Unused land	3 (~0.00%)	2 (~0.00%)	0 (0.00%)	0 (0.00%)	0 (0.00%)	0 (0.00%)	5 (~0.00%)
Total	77,369 (55.38%)	31,997 (22.90%)	8308 (5.95%)	7350 (5.27%)	14657 (10.49%)	25 (0.01%)	139,706 (100%)

Figure 9 shows the superposition analysis of EVI trends and land-use change. In terms of land-use change in areas of EVI increase (Figure 9a), 27.8% (20.5% of the total study area) was related to changes in land-use type, while 72.2% (53.4% of the total study area) was not. Of this 27.8%, the primary cause of EVI increase was transfer from "other" land use to farmland and woodland. Transfer from "other" land use to farmland mainly occurred in the plain areas of north and central Anhui, while transfer from "other" to woodland mainly occurred in the western part of central Anhui and the mountainous areas of southern Anhui.

In terms of land-use change in areas of EVI decrease (Figure 9b), 30.1% (7.9% of the total study area) was related to changes in land-use type, while 69.9% (18.2% of the total study area) was not. Of this 30.1% area, the primary cause of EVI decrease was transfer from farmland to construction land (13.7%), indicating that urban expansion in Anhui Province was mainly related to decreases in farmland, mainly in Fuyang, Bozhou and Huaibei cities in northern Anhui Province, and in Hefei City and the Wanjiang River urban belt.

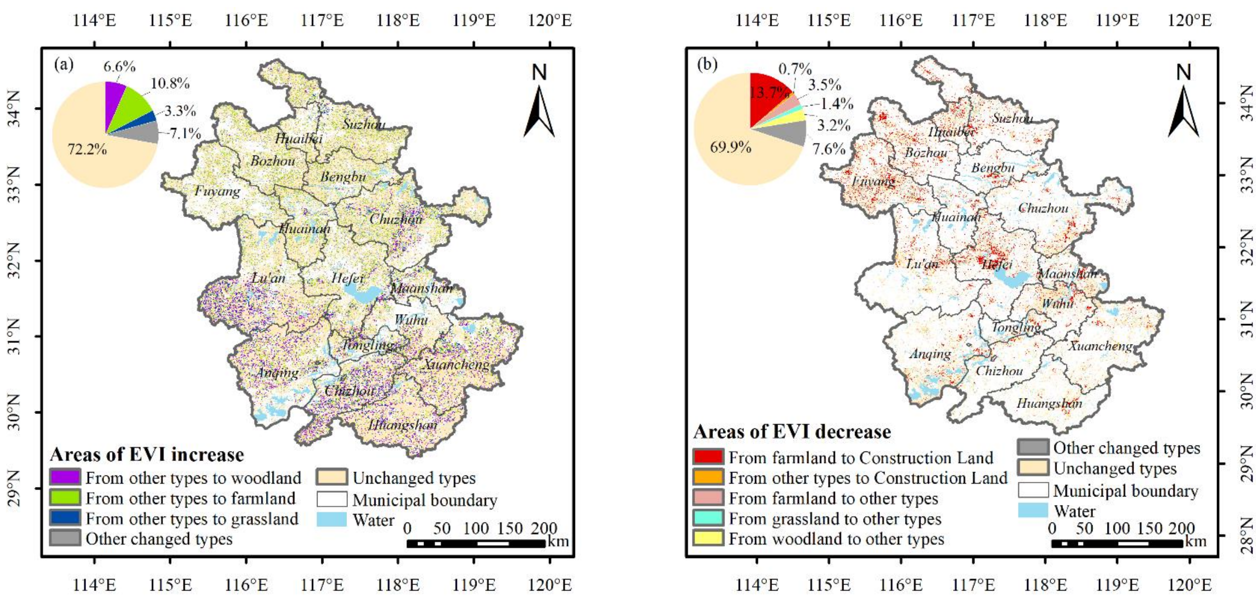

Figure 9. Superposition analysis of land-use change and Slope of EVI variation in Anhui Province. (**a**) Areas of EVI increase and (**b**) decrease.

EVI changes of different land use types transferred was quantified at the pixel-scale (Figure 10). It was obtained by subtracting the EVI data for 2000 from that for 2020 and then calculating the EVI changes caused by changes in land-use type at the pixel-scale. The results show that changes in land-use type increased the EVI, except for the transfers of farmland, woodland, grassland and construction land to unused land, which resulted in EVI decreases. Among the pixels where land-use type changed, the transfer of unused land to farmland, of construction land to woodland, of grassland to farmland and woodland, of woodland to farmland and grassland and of farmland to woodland and grassland resulted in larger increases in the EVI compared to the transfer of other land use types, corresponding to 0.08, 0.06, 0.06, 0.06, 0.06, 0.06, 0.06 and 0.06. The EVIs of farmland, woodland and grassland also increased significantly in pixels where the land use type did not transfer, by 0.04, 0.06 and 0.06, respectively. These areas were considered to be related to projects that return farmland to forest. Furthermore, with the modernization of agriculture, crop yields have increased.

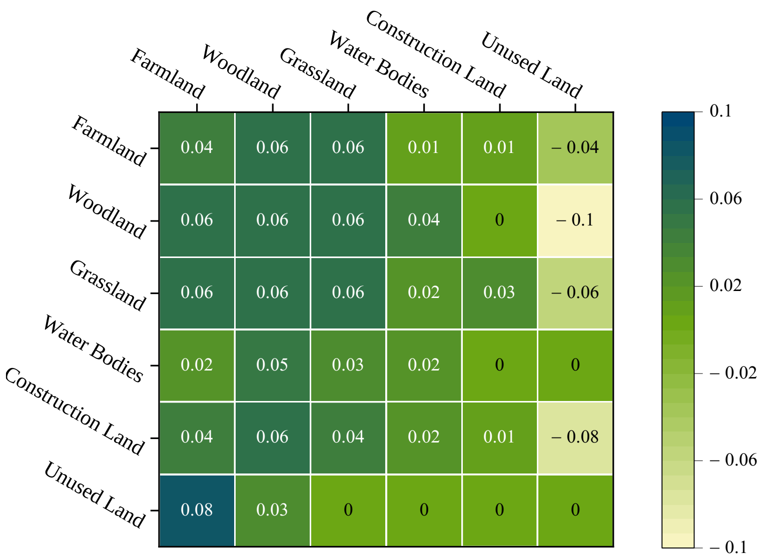

Figure 10. EVI changes of different land use types transferred in Anhui Province from 2000 to 2020 on pixel scale.

3.3. SEM of EVI Variation in Anhui Province

The final constructed SEM of the factors influencing EVI variation in Anhui Province is shown in Figure 11. All the fitting optimization indicators of the model met the requirements (CFI = 0.99, GFI = 0.99, IFI = 0.99, RMSEA = 0.05, SRMR = 0.02), indicating that the SEM was a good fit to the data.

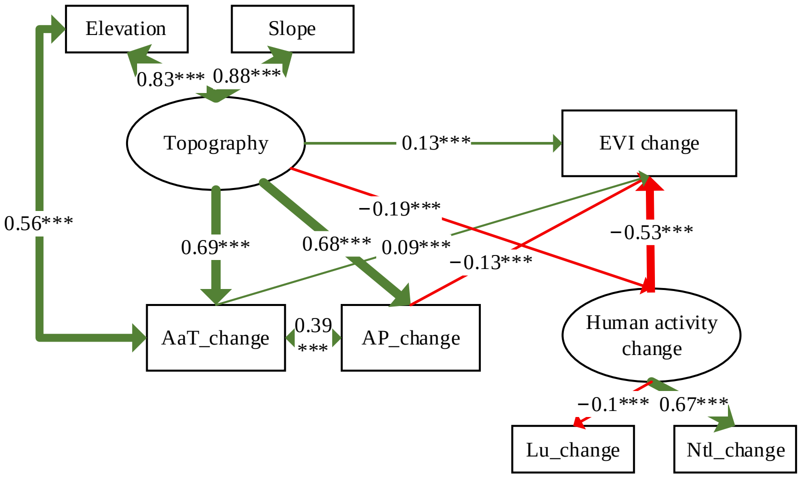

Figure 11. SEM of the relationship between EVI change and its drivers in Anhui Province. Note: AaT_change = annual average temperature change; AP_change = annual precipitation change; Lu_change = Land use change; Ntl_change = nighttime light change. Green lines represent positive effects; red lines represent negative effects. Solid lines represent significant paths. *** Significant at the 99% level.

The SEM showed that annual average temperature (AaT_change), annual precipitation (AP_change) and human activity changes only had direct effects on EVI variations, with impact coefficients of 0.09, −0.13 and −0.53, respectively. Topography not only had direct but also indirect effects on EVI variations, and their influence paths were (1) topography directly affected EVI variations with an impact factor of 0.13; (2) topography indirectly affected EVI variations by influencing annual average temperature changes, with an influence coefficient of about 0.06 ($0.69 \times 0.09 = 0.06$); (3) topography indirectly affected EVI variations by influencing annual precipitation changes, with an influence coefficient of about −0.09 and (4) topography indirectly affected EVI variations by influencing human activity changes, and the influence coefficient was about 0.1. Therefore, the total effect of topography on EVI change was 0.2 ($0.13 + 0.06 - 0.09 + 0.1 = 0.2$). Among them, there were significant interactions between elevation and annual average temperature change and between annual average temperature change and annual precipitation change, with coefficients of 0.56 and 0.39, respectively.

Statistics on the total effect of each driving factor on EVI variations showed that human activity changes had the greatest effect, followed by topography, while annual average temperature and annual precipitation changes had the least effects. Among the human activity factors, nighttime light change could better measure the effect of human activity change on EVI variation, indicating that accelerated urbanization was the primary contributor to the decreases in the EVI in Anhui Province.

3.4. SEM of EVI Variations in Northern, Central and Southern Anhui

The final SEMs of the drivers of EVI variations in northern, central and southern Anhui are shown in Figure 12. All the fitting optimization indicators of the models met the requirements (Table 5), and the model fits were good.

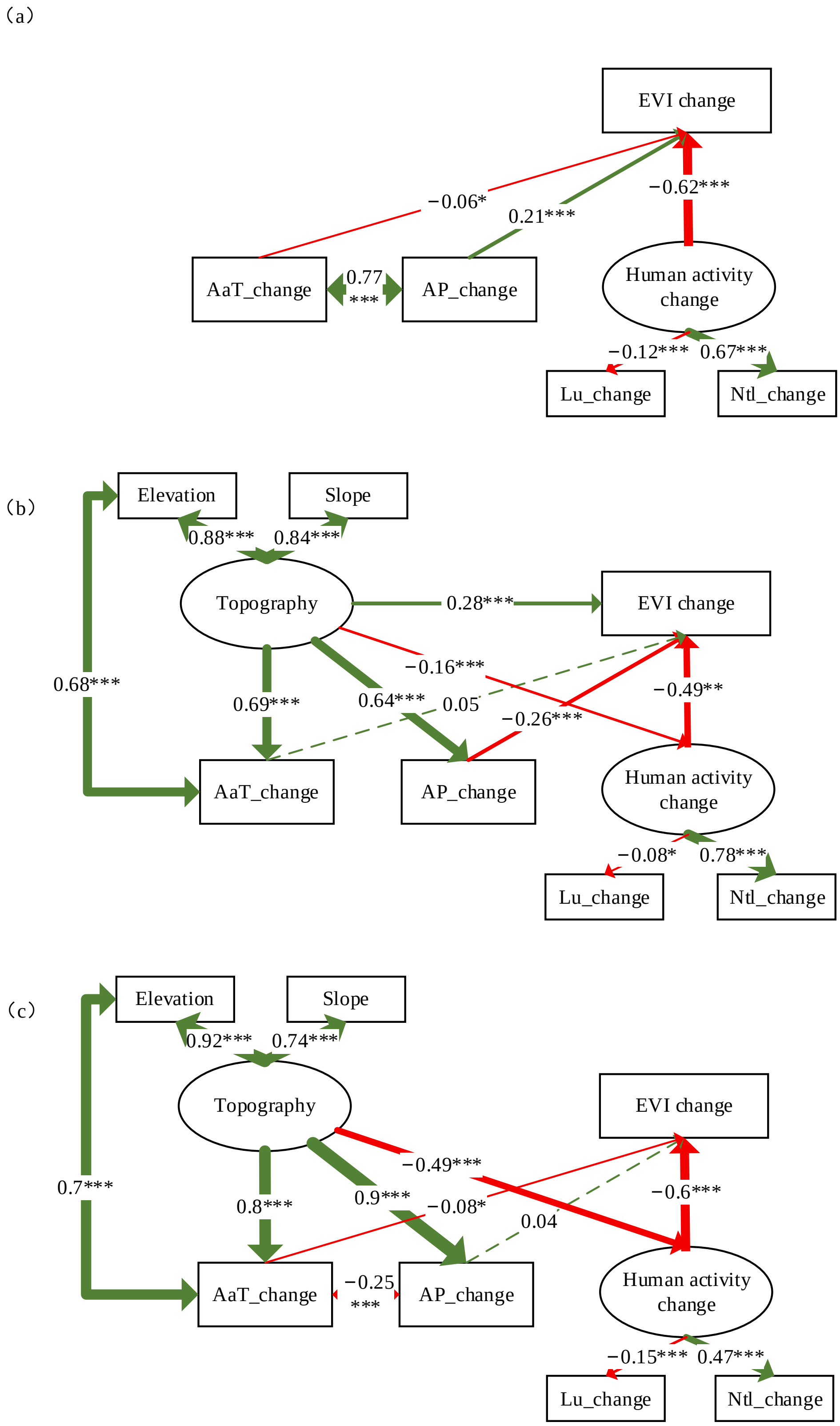

Figure 12. SEM of the relationship between EVI change and its drivers in (**a**) Northern, (**b**) Central and (**c**) Southern Anhui Province. Note: AaT_change = annual average temperature change; AP_change = annual precipitation change; Lu_change = Land use change; Ntl_change = nighttime light change. Green lines represent positive effects; red lines represent negative effects. Solid lines represent significant paths. *** Significant at the 99% level; ** Significant at the 95% level; * Significant at the 90% level.

Table 5. Structural equation model fitting results.

Fitting Optimization Index	Adaptation Standard	Evaluation Values for Each Region		
		Northern Anhui	Central Anhui	Southern Anhui
CFI	>0.90	1.00	0.98	0.99
GFI	>0.90	1.00	0.99	0.99
IFI	>0.90	1.00	0.98	0.99
RMSEA	<0.08	0.01	0.07	0.06
SRMR	<0.05	0.01	0.02	0.03

Figure 12a shows the SEM of the factors driving EVI change in northern Anhui. The model shows that EVI changes were basically unaffected by topography, while annual average temperature, annual precipitation and human activity changes had direct effects, with coefficients of −0.06, 0.21 and −0.62, respectively (Table 6). Figure 12b shows the SEM for central Anhui. The relationship between EVI changes and its drivers in central Anhui is most similar to that of the entire Anhui Province (Figure 11). The total influences of topography, annual average temperature, annual precipitation and human activity changes on EVI variations were 0.22, 0.05, −0.26 and −0.49, respectively (Table 6). Figure 12c shows the SEM for southern Anhui. Of these, topography had basically no direct effect but would have had an indirect negative effect by promoting warmer temperatures (−0.06), an indirect positive effect by increasing precipitation (0.04), and an indirect positive effect by suppressing increased human activities (0.29), resulting in a total effect of 0.27 (Table 6). Annual average temperature, annual precipitation and human activity changes only had direct effects on EVI variations, with coefficients of −0.08, 0.04 and −0.6, respectively (Table 6).

Table 6. The total impact of drivers on EVI variation in each district of Anhui Province.

Driving Factors	Northern Anhui	Central Anhui	Southern Anhui
Topography	0	0.22	0.27
AaT_change	−0.06	0.05	−0.08
AP_change	0.21	−0.26	0.04
Human activity change	−0.62	−0.49	−0.60

Although the driving mechanisms of EVI changes in northern, central and southern Anhui were different (for example, the effects of annual average temperature and annual precipitation changes on EVI variations in northern and central Anhui were stronger than those in southern Anhui (Table 6)), human activity change was the most important driving factor on EVI variation in each district of Anhui Province.

4. Discussion

4.1. Spatial and Temporal Variations in the EVI

Temporally, the EVI of Anhui Province showed an overall fluctuating increasing trend from 2000 to 2020 ($0.0181 \cdot 10a^{-1}$; Figure 3). The EVI in northern Anhui had a significant decreasing trend from 2002 to 2003, while the trends in central and southern Anhui were smaller. The EVIs in northern and central Anhui had significantly increasing trends from 2003 to 2004, while the trend in southern Anhui was smaller (Figure 3). China launched a project for returning farmland to forest in 2002, in which 17 cities in Anhui Province participated. The main construction period was 2002–2003, and by 2004, 2170.53 km^2 of farmland had been returned to forest, and 2581.67 km^2 of barren hills and wastelands were reforested. Poor-quality cultivated land that ceased to be cultivated might be the main reason for the EVI decrease in northern Anhui in 2002–2003, while the return of farmland to forest was the main reason for the EVI increase in northern and central Anhui in 2003–2004. In addition, the EVIs in northern and central Anhui also increased significantly from 2013 to 2014, which may be related to the "Ten Million Mu Forest Growth Project" implemented in Anhui Province in October 2012.

Spatially, the EVIs in Anhui Province were highest in the north and Dabie mountainous area of central Anhui and in the mountainous areas of southern Anhui and then, in the central Anhui plain and in urban areas (Figure 4). This was related to the spatial distribution of land-use types. The vegetation cover differed according to surface type and was ranked from high to low as woodland > grassland > farmland > town [43]. The mountainous area of south Anhui and the Dabie mountainous area of central Anhui were dominated by woodland, while the plain of north Anhui was dominated by farmland.

4.2. Drivers of EVI Variation

4.2.1. Topographic Factors

Topography not only affected vegetation cover changes directly but also influenced temperature, precipitation and human activities to various degrees, thus affecting vegetation changes [4]. However, most previous studies have only examined the direct effects of topography on vegetation cover change [49,50], without considering indirect effects. On the one hand, topography directly affected the spatial distribution of land-use types. There were obvious differences in vegetation type according to altitude in Anhui Province; below 200 m, the vegetation was dominated by farmland. With increases in altitude, a higher-EVI vegetation type, such as woodland or grassland, dominated [43]. On the other hand, topography could affect vegetation growth by changing the hydrothermal conditions [4]. For example, the higher the altitude or slope, the faster the annual average temperature and annual precipitation increases (Figures 11 and 12). In addition, slope can affect vegetation growth by altering surface runoff and, usually, the steeper the slope, the lower the vegetation cover [51]. However, in this study, steeper slopes had greater increases in EVI, which was due to the fact that gentle slopes were more negatively affected by human activities, while steep slopes were less affected by human activities, which is consistent with the findings of Yi et al. [52] for the middle reaches of the Yangtze River. From Figure 12, we can see that EVI variations in northern Anhui were basically uninfluenced by topography, while those in southern Anhui were highly influenced, which mainly increased EVI by suppressing human activities. This is mainly because northern Anhui is a plain area with flat topography, while southern Anhui is mostly mountainous with more complex topography.

4.2.2. Climate Factors

In the context of global warming, it is widely believed that higher temperatures will positively affect vegetation growth and enhance photosynthesis [53]; however, high temperatures will also accelerate the evaporation of soil water, reducing soil water content and leading to EVI losses [54]. In arid and semi-arid areas, water increases vegetation growth, but in humid areas with sufficient precipitation, its effect on EVI is not obvious, and excessive precipitation can even lead to soil erosion, inhibited vegetation growth and lower EVI [55,56].

From 2000 to 2020, the annual average temperature change mainly affected EVI variations in Anhui Province via interaction with the elevation and annual precipitation change, while its direct effect on EVI variations was small (Figures 11 and 12). The EVI variations in northern and central Anhui were strongly influenced by precipitation (0.211 and -0.26), while those in southern Anhui were basically unaffected by precipitation (0.04; Figure 12). There are two main reasons for this. One is that northern Anhui is in a warm temperate semi-humid climate zone, while central and southern Anhui are in a subtropical humid climate zone. Southern Anhui has the most precipitation, followed by central Anhui and then northern Anhui. Thus, EVI variations in northern Anhui are more sensitive to precipitation changes, and because precipitation in northern Anhui is relatively low, higher precipitation would increase vegetation growth and EVI, while precipitation in central Anhui is sufficient, so excessive precipitation would erode the soil and decrease vegetation growth and EVI.

The other reason is that the main land-use type in northern and central Anhui is farmland, while that in southern Anhui is mainly woodland, with farmland being more susceptible to climate change [57]. Overall, this study shows that climate had a small influence on EVI variations in Anhui Province, with human activities being the main influencing factor. This is consistent with Yang et al.'s [42] study on the drivers of NPP (Net Primary Productivity) in Anhui Province, and there have been similar findings in other regions [19].

4.2.3. Human Activity Factors

With rapid economic development, the impact of human activities on vegetation cover dynamics has become increasingly significant [58,59]. This is mainly manifested in two aspects: (1) unreasonable human farming and urban expansion will degrade vegetation, while (2) the implementation of ecological engineering projects will improve vegetation [60].

We quantified the effects of topography, climate change and human activity change on EVI variations in Anhui Province based on SEM, finding that human activity changes (land-use and nighttime light) are the main controls on vegetation cover increases and decreases (Figures 11 and 12), which is consistent with the findings of Yuan et al. [61] and Qu et al. [62] for the Yangtze River Delta region. In general, human activity change had a negative effect on EVI variations, which was mainly reflected in rapid urbanization converting large amounts of farmland into construction land. This was confirmed by Yang et al. [42] in their study of NPP variations in Anhui Province. This process mainly occurred in Fuyang, Bozhou, Huaibei, Suzhou, Fuyang, Hefei and the Wanjiang River urban belt (Figure 9b). As shown in Figure 6, areas of greater fluctuation largely coincided with areas of urban expansion. In particular, Hefei, the capital city of Anhui Province, officially joined the Yangtze River Delta region in 2010 and became a sub-center city of the Yangtze River Delta city cluster. In 2013, Hefei city joined the "Middle Four Corners" to the west and formed the Middle Yangtze River City Cluster with Wuhan, Changsha and Nanchang, which led to rapid economic development and gradual expansion of the city. On the other hand, human activity change had a positive impact on EVI variations. The study by Qu et al. [63] on the Yangtze River Basin also found that land-use changes related to ecological restoration projects were the main driver of vegetation improvement in the Yangtze River Basin. From 2000 to 2020, a series of ecological projects were implemented in Anhui Province; for example, an ecological project for returning farmland to forests was launched in 2002, while the "Ten Million Mu of Forest Growth Project" was launched in 2012 in Anhui Province. From 2000 to 2020, areas that changed from the "other" land-use type to woodland and caused an increase in EVI accounted for 4.9% of Anhui Province (Figures 5a and 9a). These mainly occurred in southern Lu'an, northern Anqing, Chuzhou, Chizhou, Huangshan and Xuancheng. In particular, from 2000 to 2020, the afforestation areas of Anqing, Chuzhou, Chizhou and Huangshan increased from 124.78 km^2, 56.87 km^2, 88.26 km^2 and 76.36 km^2 to 294.08 km^2, 200.38 km^2, 164.24 km^2 and 256.41 km^2, respectively, which largely contributed to the increase in EVI in the region.

4.3. Advantages of SEM

In this study, the effects of topography, annual average temperature change, annual precipitation change and human activity change on EVI change were quantitatively analyzed based on SEM. Compared with other study methods, SEM quantitatively identifies the interactions among variables and the direct and indirect effects on EVI variations, providing a clearer understanding of the driving mechanisms.

Figure 13 shows a correlation analysis between the EVI variations and each influencing factor for the entire Anhui Province and for northern, central and southern Anhui. The highest correlation coefficient with EVI change was nighttime light change. Followed by elevation, slope and annual average temperature changes in central and southern Anhui. However, SEM showed that the annual average temperature change had a small effect on EVI change in all regions of Anhui Province. This is mainly because the correlation analysis only estimates the correlation between two variables and does not consider the interaction between other variables. In contrast, SEM can consider complex interactions between multiple variables and estimate the relationship between two variables by excluding the effects of other variables. In this study, there were significant interactions between elevation, annual average temperature change and annual precipitation change. In addition, SEM allowed quantitative estimation of the direct and indirect effects of each driving factor (topography, annual average temperature, annual precipitation and human activity changes) on EVI variation, thus obtaining the total effect of each one. In conclusion, this study differs from existing studies on the drivers on vegetation cover dynamics. It analyzed the drivers of vegetation cover change in Anhui Province from a new perspective, proposing an innovative research framework and making up for the shortcomings in the quantitative analyses used in existing studies. The results of the study have important implications for ecological environmental protection and sustainable development in Anhui Province.

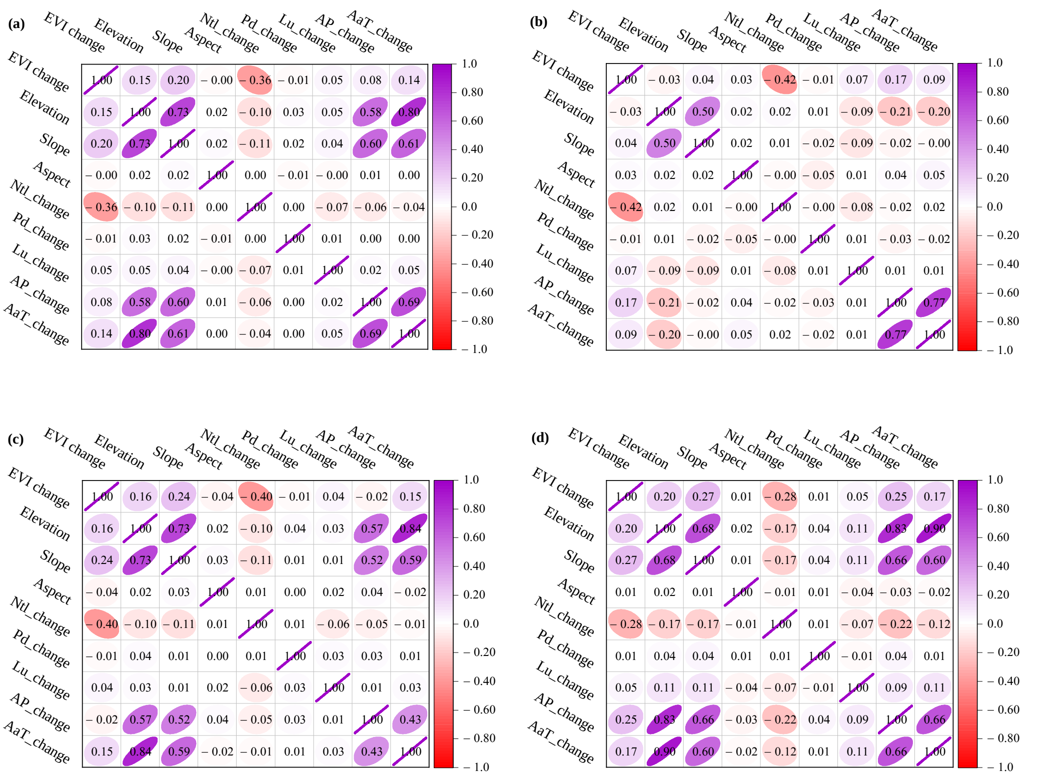

Figure 13. Pearson correlations of EVI variation and its potential drivers in (**a**) Anhui Province and (**b**) Northern, (**c**) Central and (**d**) Southern Anhui. Note: AaT_change = annual average temperature change; AP_change = annual precipitation change; Lu_change = Land use change; Ntl_change = nighttime light change.

4.4. Limitations of This Study

This study also has some limitations. First, both the NDVI and EVI are influenced by atmospheric and soil backgrounds, etc. However, compared to the NDVI, the EVI further reduces the influence of soil background and atmosphere on the basis of maintaining the advantages of the NDVI, and it has higher sensitivity and superiority for monitoring vegetation dynamics in areas with high vegetation cover [14]. Particularly, the EVI reduces the atmospheric influence on the vegetation index by introducing a blue band, which is more sensitive to atmospheric influence, to correct the red band, which is influenced by aerosol [15,64]. Meanwhile, this study used land use data with a spatial resolution of 1 km to analyze the effect of land-use change on vegetation-cover change. This resolution may be a bit low for the analysis of construction land; however, our study period spanned 21 years, and the expansion of construction land was much larger than 1 km; therefore, we believe that the resolution of this data does not affect the analysis results of this study. It should also be noted that the effect of climate change on vegetation change is lagged [65,66] but to different extents depending on the geographical environment and vegetation types. Hence, there is no uniform selection standard for the lag interval. The geographical location of Anhui Province is special, and the differences in vegetation types between southern and northern Anhui are obvious. Therefore, to prevent errors due to the unreasonable selection of time lag intervals, the lagged effect of climate change on vegetation change was not considered in this paper. In addition, the selection of the potential influences on vegetation cover change was not comprehensive enough, and the quantification of human activity factors is challenging because of a lack of available data, especially in areas with strong human activity [4]. Therefore, high resolution data will be considered for use in future studies, and the study area will be further refined to fully consider the effects of multiple factors on vegetation cover change and obtain a clearer understanding of the mechanisms driving vegetation cover change.

5. Conclusions

This study analyzed the characteristics of spatial and temporal variations in EVI in Anhui Province using MOD13Q1 EVI data acquired from 2000 to 2020. It explored the influences on EVI variations using land-use data from 2000 and 2020 and, finally, quantified the effects of topography (elevation, slope and aspect), annual average temperature change, annual precipitation change and human activity change (population density change, nighttime light change and land-use change) on EVI variations based on SEM. The following main conclusions were obtained:

(1) Temporally, the EVI of Anhui Province showed a trend of a fluctuating increase at a rate of $0.0181 \cdot 10a^{-1}$ between 2000 and 2020.

(2) The EVI in Anhui Province showed a spatial distribution pattern of being high in the north and south and low in the middle. The spatial trend in EVI was dominated by improvement, with 64.2% of the regions having significant improvements in EVI. The fluctuation in EVI variation in most regions of the province was extremely low and low. High fluctuations occurred in urban areas. After 2020, the EVI is likely to decrease, so the government should strengthen relevant vegetation greening and protection measures.

(3) Among the areas where EVI increased, 10.8% of the areas was transferred from "other" land use to farmland, mainly in the northern and central Anhui plain areas. Some 6.6% were transferred from "other" land use to woodland, mainly in the mountainous area of central and southern Anhui. Among the regions with reduced EVI, 13.7% was transferred from farmland to construction land, mainly in Hefei, Fuyang, Bozhou, Huaibei, and the Wanjiang River urban belt. Therefore, the government needs to pay special attention to the coordinated development of accelerated urbanization and ecological environmental protection.

(4) The SEM showed that human activity changes (mainly nighttime light change) were the main cause of EVI decreases in Anhui Province. Except for northern Anhui, central and southern Anhui were affected by the complexity of the topography. In addition, the EVI variations in Anhui Province were less influenced by annual average temperature change, and the influence of annual precipitation change showed that northern and central Anhui were higher than southern Anhui.

Author Contributions: Conceptualization, Z.Z.; methodology, Z.G.; software, Z.G.; validation, Z.Z.; formal analysis, Z.G. and Z.Z.; investigation, Z.G. and Z.Z.; resources, Z.G. and Z.Z.; data curation, Z.G. and L.W.; writing—original draft preparation, Z.G. and Z.Z.; writing—review and editing, Z.G., Z.Z. and J.Y.; visualization, Z.G. and J.Y.; supervision, Z.Z.; project administration, L.W.; funding acquisition, Z.Z. and L.W. All authors have read and agreed to the published version of the manuscript.

Funding: This research was funded by the National Natural Science Foundation of China (Grant Nos. 42071085 and 41701087), the Open Project of the State Key Laboratory of Cryospheric Science (Grant

No. SKLCS 2020-10) and the Graduate Scientific research project of Anhui Universities in 2021 (Grant No. YJS20210412).

Data Availability Statement: Not applicable.

Acknowledgments: We would like to thank NASA (National Aeronautics and Space Administration) for the EVI data (http://doi.org/10.5067/MODIS/MOD13Q1.006, accessed on 26 January 2022), the United States Geological Survey (https://earthexplorer.usgs.gov, accessed on 26 January 2022) for the SRTM data, the WorldPop (https://www.worldpop.org, accessed on 26 January 2022) for the population density data, the Resource and Environment Science and Data Center (http://www.resdc.cn, accessed on 26 January 2022) for the land use data, the China Meteorological Data Service Center (http://data.cma.cn, accessed on 26 January 2022) for the climate factor data and Chen et al.'s extended time series (2000–2018) of global NPP-VIIRS-like nighttime light data from a cross-sensor calibration (https://doi.org/10.7910/DVN/YGIVCD, accessed on 26 January 2022) for the Nighttime light data.

Conflicts of Interest: The authors declare no conflict of interest.

References

1. Guan, J.; Yao, J.; Li, M.; Zheng, J. Assessing the Spatiotemporal Evolution of Anthropogenic Impacts on Remotely Sensed Vegetation Dynamics in Xinjiang, China. *Remote Sens.* **2021**, *13*, 4651. [CrossRef]
2. Fan, D.; Ni, L.; Jiang, X.; Fang, S.; Wu, H.; Zhang, X. Spatiotemporal analysis of vegetation changes along the belt and road initiative region from 1982 to 2015. *IEEE Access* **2020**, *8*, 122579–122588. [CrossRef]
3. Liu, S.; Huang, S.; Xie, Y.; Wang, H.; Huang, Q.; Leng, G.; Li, P.; Wang, L. Spatial-temporal changes in vegetation cover in a typical semi-humid and semi-arid region in China: Changing patterns, causes and implications. *Ecol. Indic.* **2019**, *98*, 462–475. [CrossRef]
4. Liu, C.; Li, W.; Wang, W.; Zhou, H.; Liang, T.; Hou, F.; Xu, J.; Xue, P. Quantitative spatial analysis of vegetation dynamics and potential driving factors in a typical alpine region on the northeastern Tibetan Plateau using the Google Earth Engine. *Catena* **2021**, *206*, 105500. [CrossRef]
5. Yang, K.; Sun, W.; Luo, Y.; Zhao, L. Impact of urban expansion on vegetation: The case of China (2000–2018). *J. Environ. Manag.* **2021**, *291*, 112598. [CrossRef]
6. Jiang, M.; He, Y.; Song, C.; Pan, Y.; Qiu, T.; Tian, S. Disaggregating climatic and anthropogenic influences on vegetation changes in Beijing-Tianjin-Hebei region of China. *Sci. Total Environ.* **2021**, *786*, 147574. [CrossRef]
7. Kang, Y.; Guo, E.; Wang, Y.; Bao, Y.; Bao, Y.; Mandula, N. Monitoring Vegetation Change and Its Potential Drivers in Inner Mongolia from 2000 to 2019. *Remote Sens.* **2021**, *13*, 3357. [CrossRef]
8. Feng, D.; Fu, M.; Sun, Y.; Bao, W.; Zhang, M.; Zhang, Y.; Wu, J. How Large-Scale Anthropogenic Activities Influence Vegetation Cover Change in China? A Review. *Forests* **2021**, *12*, 320. [CrossRef]
9. Ali, S.; Tong, D.; Xu, Z.; Henchiri, M.; Wilson, K.; Siqi, S.; Zhang, J. Characterization of drought monitoring events through MODIS and TRMM-based DSI and TVDI over South Asia during 2001–2017. *Environ. Sci. Pollut. Res.* **2021**, *28*, 21085–21100. [CrossRef]
10. Liu, Q.; Zhang, J.; Zhang, H.; Yao, F.; Bai, Y.; Zhang, S.; Meng, X.; Liu, Q. Evaluating the performance of eight drought indices for capturing soil moisture dynamics in various vegetation regions over China. *Sci. Total Environ.* **2021**, *789*, 147803. [CrossRef]
11. Ren, Y.; Liu, J.; Liu, S.; Wang, Z.; Liu, T.; Shalamzari, M.J. Effects of Climate Change on Vegetation Growth in the Yellow River Basin from 2000 to 2019. *Remote Sens.* **2022**, *14*, 687. [CrossRef]
12. Shi, S.; Wang, P.; Zhang, Y.; Yu, J. Cumulative and time-lag effects of the main climate factors on natural vegetation across Siberia. *Ecol. Indic.* **2021**, *133*, 108446. [CrossRef]
13. Li, J.; Peng, S.; Li, Z. Detecting and attributing vegetation changes on China's Loess Plateau. *Agric. For. Meteorol.* **2017**, *247*, 260–270. [CrossRef]
14. Diao, C.; Liu, Y.; Zhao, L.; Zhuo, G.; Zhang, Y. Regional-scale vegetation-climate interactions on the Qinghai-Tibet Plateau. *Ecol. Inform.* **2021**, *65*, 101413. [CrossRef]
15. Huete, A.; Didan, K.; Miura, T.; Rodriguez, E.P.; Gao, X.; Ferreira, L.G. Overview of the radiometric and biophysical performance of the MODIS vegetation indices. *Sci. Total Environ.* **2002**, *83*, 195–213. [CrossRef]
16. Liu, H.; Li, X.; Mao, F.; Zhang, M.; Zhu, D.; He, S.; Huang, Z.; Du, H. Spatiotemporal evolution of fractional vegetation cover and its response to climate change based on MODIS data in the subtropical region of China. *Remote Sens.* **2021**, *13*, 913. [CrossRef]
17. Liu, H.; Liu, F.; Yuan, H.; Zheng, L.; Zhang, Y. Assessing the relative role of climate and human activities on vegetation cover changes in the up–down stream of Danjiangkou, China. *J. Plant Ecol.* **2022**, *15*, 180–195. [CrossRef]
18. Jiang, W.; Niu, Z.; Wang, L.; Yao, R.; Gui, X.; Xiang, F.; Ji, Y. Impacts of Drought and Climatic Factors on Vegetation Dynamics in the Yellow River Basin and Yangtze River Basin, China. *Remote Sens.* **2022**, *14*, 930. [CrossRef]
19. Liu, Z.; Liu, Y.; Li, Y. Anthropogenic contributions dominate trends of vegetation cover change over the farming-pastoral ecotone of northern China. *Ecol. Indic.* **2018**, *95*, 370–378. [CrossRef]
20. Xue, L.; Kappas, M.; Wyss, D.; Wang, C.; Putzenlechner, B.; Thi, N.P.; Chen, J. Assessment of climate change and human activities on vegetation development in Northeast China. *Sensors* **2022**, *22*, 2509. [CrossRef]

21. Deng, X.; Hu, S.; Zhan, C. Attribution of vegetation coverage change to climate change and human activities based on the geographic detectors in the Yellow River Basin, China. *Environ. Sci. Pollut. Res.* **2022**, *29*, 44693–44708. [CrossRef] [PubMed]
22. Wang, G.; Peng, W. Quantifying spatiotemporal dynamics of vegetation and its differentiation mechanism based on geographical detector. *Environ. Sci. Pollut. Res.* **2022**, *29*, 32016–32031. [CrossRef] [PubMed]
23. Leroux, L.; Bégué, A.; Seen, D.L.; Jolivot, A.; Kayitakire, F. Driving forces of recent vegetation changes in the Sahel: Lessons learned from regional and local level analyses. *Sci. Total Environ.* **2017**, *191*, 38–54. [CrossRef]
24. Bafitlhile, T.M.; Liu, Y. Temperature contributes more than precipitation to the greening of the Tibetan Plateau during 1982–2019. *Theor. Appl. Climatol.* **2022**, *147*, 1471–1488. [CrossRef]
25. Xue, J.; Wang, Y.; Teng, H.; Wang, N.; Li, D.; Peng, J.; Biswas, A.; Shi, Z. Dynamics of Vegetation Greenness and Its Response to Climate Change in Xinjiang over the Past Two Decades. *Remote Sens.* **2021**, *13*, 4063. [CrossRef]
26. Na, R.; Na, L.; Du, H.; He, H.S.; Shan, Y.; Zong, S.; Huang, L.; Yang, Y.; Wu, Z. Vegetation Greenness Variations and Response to Climate Change in the Arid and Semi-Arid Transition Zone of the Mongo-Lian Plateau during 1982–2015. *Remote Sens.* **2021**, *13*, 4066. [CrossRef]
27. Tang, Z.; Ma, J.; Peng, H.; Wang, S.; Wei, J. Spatiotemporal changes of vegetation and their responses to temperature and precipitation in upper Shiyang river basin. *Adv. Space Res.* **2017**, *60*, 969–979. [CrossRef]
28. Liu, Y.; Tian, J.; Liu, R.; Ding, L. Influences of Climate Change and Human Activities on NDVI Changes in China. *Remote Sens.* **2021**, *13*, 4326. [CrossRef]
29. Shi, S.; Yu, J.; Wang, F.; Wang, P.; Zhang, Y.; Jin, K. Quantitative contributions of climate change and human activities to vegetation changes over multiple time scales on the Loess Plateau. *Sci. Total Environ.* **2021**, *755*, 142419. [CrossRef] [PubMed]
30. Zhang, Y.; He, Y.; Li, Y.; Jia, L. Spatiotemporal variation and driving forces of NDVI from 1982 to 2015 in the Qinba Mountains, China. *Environ. Sci. Pollut. Res.* **2022**, *29*, 52277–52288. [CrossRef]
31. Zhang, M.; Du, H.; Zhou, G.; Mao, F.; Li, X.; Zhou, L.; Zhu, D.; Xu, Y.; Huang, Z. Spatiotemporal Patterns and Driving Force of Urbanization and Its Impact on Urban Ecology. *Remote Sens.* **2022**, *14*, 1160. [CrossRef]
32. Yang, W.; Zhao, Y.; Wang, Q.; Guan, B. Climate, CO_2, and Anthropogenic Drivers of Accelerated Vegetation Greening in the Haihe River Basin. *Remote Sens.* **2022**, *14*, 268. [CrossRef]
33. Xiong, Y.; Li, Y.; Xiong, S.; Wu, G.; Deng, O. Multi-scale spatial correlation between vegetation index and terrain attributes in a small watershed of the upper Minjiang River. *Ecol. Indic.* **2021**, *126*, 107610. [CrossRef]
34. Wang, J.; Sun, H.; Xiong, J.; He, D.; Cheng, W.; Ye, C.; Yong, Z.; Huang, X. Dynamics and drivers of vegetation phenology in three-river headwaters region based on the Google Earth engine. *Remote Sens.* **2021**, *13*, 2528. [CrossRef]
35. Hou, D.; Al-Tabbaa, A.; Chen, H.; Mamic, I. Factor analysis and structural equation modelling of sustainable behaviour in contaminated land remediation. *J. Clean. Prod.* **2014**, *84*, 439–449. [CrossRef]
36. Li, Z.; Han, X.; Lin, X.; Lu, X. Quantitative analysis of landscape efficacy based on structural equation modelling: Empirical evidence from new Chinese style commercial streets. *Alex. Eng. J.* **2021**, *60*, 261–271. [CrossRef]
37. Pearl, J. The causal mediation formula—A guide to the assessment of pathways and mechanisms. *Prev. Sci.* **2012**, *13*, 426–436. [CrossRef]
38. Liu, C.; Zhang, F.; Wang, X.; Chan, N.W.; Rahman, H.A.; Yang, S.; Tan, M.L. Assessing the factors influencing water quality using environment water quality index and partial least squares structural equation model in the Ebinur Lake Watershed, Xinjiang, China. Environ. *Sci. Pollut. Res.* **2022**, *29*, 29033–29048. [CrossRef]
39. Urbach, N.; Ahlemann, F. Structural equation modeling in information systems research using partial least squares. *J. Inf. Technol. Theory Appl.* **2010**, *11*, 5–40.
40. Shao, W.; Wang, Q.; Guan, Q.; Luo, H.; Ma, Y.; Zhang, J. Distribution of soil available nutrients and their response to environmental factors based on path analysis model in arid and semi-arid area of northwest China. *Sci. Total Environ.* **2022**, *827*, 154254. [CrossRef]
41. Hao, J.; Xu, G.; Luo, L.; Zhang, Z.; Yang, H.; Li, H. Quantifying the relative contribution of natural and human factors to vegetation coverage variation in coastal wetlands in China. *Catena* **2020**, *188*, 104429. [CrossRef]
42. Yang, H.; Hu, D.; Xu, H.; Zhong, X. Assessing the spatiotemporal variation of NPP and its response to driving factors in Anhui province, China. Environ. *Sci. Pollut. Res.* **2020**, *27*, 14915–14932. [CrossRef]
43. Yao, Z.; Wu, D.; Chu, R.; Yao, Y.; He, B.; Huang, Y. Dynamic change of vegetation coverage and its response to topography in Anhui Province. Bull. *Soil Water Conserv.* **2021**, *41*, 283–290.
44. Chen, Z.; Yu, B.; Yang, C.; Zhou, Y.; Yao, S.; Qian, X.; Wang, C.; Wu, B.; Wu, J. An extended time series (2000–2018) of global NPP-VIIRS-like nighttime light data from a cross-sensor calibration. *Earth Syst. Sci. Data* **2021**, *13*, 889–906. [CrossRef]
45. Ma, B.; Wang, S.; Mupenzi, C.; Li, H.; Ma, J.; Li, Z. Quantitative contributions of climate change and human activities to vegetation changes in the Upper White Nile River. *Remote Sens.* **2021**, *13*, 3648. [CrossRef]
46. Gu, Z.; Duan, X.; Shi, Y.; Li, Y.; Xi, P. Spatiotemporal variation in vegetation coverage and its response to climatic factors in the Red River Basin, China. *Ecol. Indic.* **2018**, *93*, 54–64. [CrossRef]
47. Hong, S.; Kim, S. Comparisons of multilevel modeling and structural equation modeling approaches to actor–partner interdependence model. *Psychol. Rep.* **2019**, *122*, 558–574. [CrossRef]
48. Zheng, H.; Miao, C.; Li, X.; Kong, D.; Gou, J.; Wu, J.; Zhang, S. Effects of vegetation changes and multiple environmental factors on evapotranspiration across China over the past 34 years. *Earth's Future* **2022**, *10*, e2021EF002564. [CrossRef]

49. Peng, W.; Kuang, T.; Tao, S. Quantifying influences of natural factors on vegetation NDVI changes based on geographical detector in Sichuan, western China. *J. Clean. Prod.* **2019**, *233*, 353–367. [CrossRef]
50. Zhang, Y.; Xu, G.; Li, P.; Li, Z.; Wang, Y.; Wang, B.; Jia, L.; Cheng, Y.; Zhang, J.; Zhuang, S.; et al. Vegetation change and its relationship with climate factors and elevation on the Tibetan plateau. *Int. J. Environ. Res. Public Health* **2019**, *16*, 4709. [CrossRef]
51. Gao, S.; Dong, G.; Jiang, X.; Nie, T.; Yin, H.; Guo, X. Quantification of Natural and Anthropogenic Driving Forces of Vegetation Changes in the Three-River Headwater Region during 1982–2015 Based on Geographical Detector Model. *Remote Sens.* **2021**, *13*, 4175. [CrossRef]
52. Yi, Y.; Wang, B.; Shi, M.; Meng, Z.; Zhang, C. Variation in Vegetation and Its Driving Force in the Middle Reaches of the Yangtze River in China. *Water* **2021**, *13*, 2036. [CrossRef]
53. Sun, R.; Chen, S.; Su, H. Climate Dynamics of the Spatiotemporal Changes of Vegetation NDVI in Northern China from 1982 to 2015. *Remote Sens.* **2021**, *13*, 187. [CrossRef]
54. Liu, Q.; Liu, L.; Zhang, Y.; Wang, Z.; Wu, J.; Li, L.; Li, S.; Paudel, B. Identification of impact factors for differentiated patterns of NDVI change in the headwater source region of Brahmaputra and Indus, Southwestern Tibetan Plateau. *Ecol. Indic.* **2021**, *125*, 107604. [CrossRef]
55. Chen, J.; Yan, F.; Lu, Q. Spatiotemporal variation of vegetation on the Qinghai–Tibet Plateau and the influence of climatic factors and human activities on vegetation trend (2000–2019). *Remote Sens.* **2020**, *12*, 3150. [CrossRef]
56. Feng, X.; Fu, B.; Piao, S.; Wang, S.; Ciais, P.; Zeng, Z.; Lü, Y.; Zeng, Y.; Li, Y.; Jiang, X.; et al. Revegetation in China's Loess Plateau is approaching sustainable water resource limits. *Nat. Clim. Chang.* **2016**, *6*, 1019–1022. [CrossRef]
57. Deng, W.; Yuan, X.; Liu, H.; Zhang, Y.; Li, B. Influence of regional climate change on vegetation cover in the middle and lower Yangtze River basin. *Res. Environ. Sci.* **2014**, *27*, 1032–1042.
58. Díaz, S.; Pascual, U.; Stenseke, M.; Stenseke, M.; Martín-López, B.; Watson, R.T.; Molnár, Z.; Hill, R.; Chan, K.M.A.; Baste, I.A.; et al. Assessing nature's contributions to people. *Science* **2018**, *359*, 270–272. [CrossRef]
59. Zhang, X.; Huang, X. Human disturbance caused stronger influences on global vegetation change than climate change. *PeerJ* **2019**, *7*, e7763. [CrossRef]
60. He, X.; Yu, Y.; Cui, Z.; He, T. Climate Change and Ecological Projects Jointly Promote Vegetation Restoration in Three-River Source Region of China. *Chin. Geogr. Sci.* **2021**, *31*, 1108–1122. [CrossRef]
61. Yuan, J.; Xu, Y.; Xiang, J.; Wu, L.; Wang, D. Spatiotemporal variation of vegetation coverage and its associated influence factor analysis in the Yangtze River Delta, eastern China. *Environ. Sci. Pollut. Res.* **2019**, *26*, 32866–32879. [CrossRef] [PubMed]
62. Qu, S.; Wang, L.; Lin, A.; Yu, D.; Yuan, M.; Li, C. Distinguishing the impacts of climate change and anthropogenic factors on vegetation dynamics in the Yangtze River Basin, China. *Ecol. Indic.* **2020**, *108*, 105724. [CrossRef]
63. Qu, S.; Wang, L.; Lin, A.; Zhu, H.; Yuan, M. What drives the vegetation restoration in Yangtze River basin, China: Climate change or anthropogenic factors? *Ecol. Indic.* **2018**, *90*, 438–450. [CrossRef]
64. Hao, C.; Wu, S.; Xu, C. Comparison of some vegetation indices in seasonal information. *Chin. Geogr. Sci.* **2008**, *18*, 242–248. [CrossRef]
65. Cai, S.; Song, X.; Hu, R.; Guo, D. Ecosystem-Dependent Responses of Vegetation Coverage on the Tibetan Plateau to Climate Factors and Their Lag Periods. *ISPRS Int. J. Geoinf.* **2021**, *10*, 394. [CrossRef]
66. Tang, W.; Liu, S.; Kang, P.; Peng, X.; Li, Y.; Guo, R.; Jia, J.; Liu, M.; Zhu, L. Quantifying the lagged effects of climate factors on vegetation growth in 32 major cities of China. *Ecol. Indic.* **2021**, *132*, 108290. [CrossRef]